

UC Santa Barbara

UC Santa Barbara Previously Published Works

Title

Using 2D NMR spectroscopy to assess effects of UV radiation on cell wall chemistry during litter decomposition

Permalink

<https://escholarship.org/uc/item/7bn271zr>

Journal

Biogeochemistry, 125(3)

ISSN

0168-2563

Authors

Lin, Yang
King, Jennifer Y
Karlen, Steven D
[et al.](#)

Publication Date

2015-09-01

DOI

10.1007/s10533-015-0132-1

Copyright Information

This work is made available under the terms of a Creative Commons Attribution-NonCommercial-ShareAlike License, available at <https://creativecommons.org/licenses/by-nc-sa/4.0/>

Peer reviewed

1 **Using 2D NMR spectroscopy to assess effects of UV radiation on cell wall chemistry**
2 **during litter decomposition**

3 Yang Lin^{1*}, Jennifer Y. King¹, Steven D. Karlen², and John Ralph^{2,3}

4 ¹Department of Geography, University of California, Santa Barbara, CA 93106-4060,
5 USA

6 ²U.S. Department of Energy (DOE) Great Lakes Bioenergy Research Center, The
7 Wisconsin Energy Institute, University of Wisconsin-Madison, Madison, WI 53726, USA

8 ³Department of Biochemistry, University of Wisconsin-Madison, Madison, WI 53706,
9 USA

10 *Corresponding author; Tel. +1 805 893 3663; E-mail address: ylin@geog.ucsb.edu

11 Journal: *Biogeochemistry*

12 Type of manuscript: Brief Communication

13 **Abstract**

14 Litter chemistry is one of the most studied controls on decomposition in terrestrial
15 ecosystems. Solar radiation has been shown to increase litter decomposition rates in arid
16 ecosystems through the process of photodegradation. However, it remains unclear how
17 photodegradation affects litter chemistry, especially the abundance and composition of
18 lignin, which is thought to play a key role in photodegradation. Using two-dimensional
19 nuclear magnetic resonance (2D NMR) spectroscopic methods, we quantified the
20 molecular-level changes in litter chemistry associated with photodegradation. Litter of
21 *Bromus diandrus* was exposed in the field to two levels of radiation (with and without
22 ultraviolet (UV) wavelengths) and two durations of exposure (2.5 months during summer,
23 and one year). Through fiber analysis by sequential digestion, we found that the litter
24 hemicellulose fraction decreased significantly from 31.6% to 24.9% after one year of
25 decomposition. In litter exposed for one year, the hemicellulose fraction was significantly
26 lower in litter with UV exposure compared to litter without UV exposure (23.8% vs.
27 25.9%). These results indicate that UV photodegradation has a small but significant effect
28 on litter chemistry compared to other decomposition processes. Even though fiber
29 analysis showed no loss of total lignin, 2D NMR analysis demonstrated that UV exposure
30 reduced the major lignin structural units containing β -aryl ether inter-unit linkages by 9%
31 and decreased the relative abundance of lignin *p*-hydroxyphenyl units by 20%. The 2D
32 NMR analysis also revealed that lignin guaiacyl units were preferentially lost after one
33 year of decomposition relative to the reference material, but no effects of UV exposure on
34 guaiacyl were observed. These results suggest that photodegradation causes partial
35 degradation, not necessarily complete breakdown, of lignin structures. Our data also

36 demonstrate that applications of 2D NMR methods are valuable for acquiring detailed
37 information on lignin and polysaccharide chemistry during both biotic and abiotic
38 decomposition processes.

39 **Keywords**

40 photo-oxidation, photo-mineralization, photo-priming, cellulose, dryland, HSQC
41 (heteronuclear single-quantum coherence)

42 **Introduction**

43 Litter chemistry is perhaps the most studied control on litter decomposition in terrestrial
44 ecosystems (e.g. Amin et al. 2014; Bertrand et al. 2006; Melillo et al. 1982; Talbot et al.
45 2011). Together with climatic variables (i.e. temperature, precipitation, and actual
46 evapotranspiration), litter chemistry has been shown to reasonably predict litter
47 decomposition rates (Aerts 1997; Moore et al. 1999). However, models based on litter
48 chemistry and climate tend to under-estimate decomposition rates in arid ecosystems
49 (Adair et al. 2008; Parton et al. 2007; Schaefer et al. 1985). This discrepancy may be
50 explained in part by photodegradation, the process through which solar radiation
51 contributes to organic matter decomposition (reviewed by King et al. 2012).

52 Photodegradation *directly* breaks down plant litter through photochemical oxidation and
53 releases gases such as CO₂, CO, and CH₄ (Brandt et al. 2009; Lee et al. 2012; Schade et
54 al. 1999). Photodegradation also *indirectly* contributes to litter decomposition by
55 affecting litter chemistry, because solar radiation can partially degrade litter and make it
56 more vulnerable to microbial decomposition (Foereid et al. 2010; Frouz et al. 2011;
57 Wang et al. 2015). Recently, photodegradation has been suggested to influence organic
58 matter turnover in the surface soil (Mayer et al. 2012). For example, Feng et al. (2011)
59 found that photodegradation increased the solubility of soil organic matter and potentially
60 contributed to soil C loss through leaching. However, our understanding of the chemical
61 mechanisms underlying photodegradation is still incomplete.

62 Photodegradation is generally assumed to increase the breakdown of lignin (Austin
63 and Ballaré 2010; King et al. 2012; Song et al. 2013), which exhibits strong absorption of
64 both ultraviolet (UV) and shortwave visible radiation (George et al. 2005). However,

65 contradictory results have been reported with regard to changes in lignin content during
66 photodegradation of plant litter. Using the acid-detergent method (Van Soest 1963), Song
67 et al. (2014) found that exposure to UV radiation increased loss of lignin, whereas
68 Kirschbaum et al. (2011) and Lin and King (2014) found no significant change in lignin
69 content following UV exposure. Focusing on lignin content alone does not advance our
70 mechanistic understanding of the role of lignin during litter photodegradation. This
71 knowledge gap further hinders our ability to predict the contribution of photodegradation
72 to litter decomposition.

73 Recent studies have started to explore how lignin chemical composition and structure
74 change during litter photodegradation. Feng et al. (2011) found that UV photodegradation
75 increased the breakdown of aliphatic substances in corn (*Zea mays*) and loblolly pine
76 (*Pinus taeda*) litter, but photodegradation did not affect lignin-derived phenols in water-
77 extractable fractions. Frouz et al. (2011), on the other hand, found that photodegradation
78 enhanced loss of lignin syringyl units of bushgrass (*Calamagrostis epigejos*) litter. These
79 inconsistent changes in lignin chemistry in response to litter photodegradation emphasize
80 the need for more in-depth investigation of the chemical mechanisms behind
81 photodegradation.

82 New methods in solution-state nuclear magnetic resonance (NMR) spectroscopy have
83 been developed in recent years to enable rapid evaluation of lignin and polysaccharide
84 structures, even on (unfractionated) whole cell walls or whole plant material (Kim and
85 Ralph 2010; Kim et al. 2008; Mansfield et al. 2012). The swelling of ball-milled cell wall
86 material in organic solvent produces a gel that allows the use of two-dimensional (2D)
87 ^1H - ^{13}C heteronuclear single-quantum coherence (HSQC) NMR spectroscopy for

88 relatively detailed characterization of lignin and polysaccharide (Kim and Ralph 2010;
89 Mansfield et al. 2012). In principle, this 2D NMR method provides compositional
90 information on whole lignin, not the lignin components released by degradative methods,
91 such as thioacidolysis, cupric oxidation, tetramethylammonium hydroxide
92 thermochemolysis, and hydrolysis. The 2D NMR method does not degrade or alter cell
93 wall chemistry beyond sonication and ball-milling (Kim et al. 2008). Furthermore, it
94 characterizes many key features of plant cell walls, including lignin units, lignin inter-
95 unit linkages, and hemicellulose, most of which cannot be inferred from one-dimensional
96 solid-state ^{13}C NMR experiments. Integration of 2D NMR contours generates highly
97 reproducible measurements (within 5%) of cell wall components and has been used in
98 comparative studies on genetic modification of cell walls and litter decomposition (e.g.,
99 Petrik et al. 2014; Talbot et al. 2011; Wilkerson et al. 2014; Yelle et al. 2013). This
100 method also provides estimates of lignin units that are comparable to other conventional
101 methods, including thioacidolysis, nitrobenzene oxidation, and derivatization followed by
102 reductive cleavage (Mansfield et al. 2012). The method tends to overestimate the absolute
103 abundance of the terminal end units (e.g., *p*-coumarate units) because of their long
104 relaxation times compared to those of the bulk polymers. In addition, cellulose
105 abundances are underestimated in the cell wall gels because the crystalline cellulose does
106 not swell in solvent. Nevertheless, the 2D NMR method is accurate in providing
107 comparative information between samples (Mansfield et al. 2012). It has been reported to
108 offer better resolution of hemicelluloses and provides information on natural acetylation
109 that is not available in a cell wall dissolution method based on acetylation (Kim et al.
110 2008). Therefore we chose to employ the 2D NMR method to examine changes in lignin

111 and hemicellulose for litter subjected to photodegradation and other decomposition
112 processes.

113 The aim of this study was to quantify the molecular-level changes in litter chemistry
114 with photodegradation. Samples of a common grassland litter were treated with either
115 ambient or reduced UV radiation under field conditions for two durations, 2.5 months or
116 one year. Changes in lignin units, lignin inter-unit linkages, and hemicelluloses were
117 studied using 2D NMR spectroscopy. Differences in litter chemistry between the
118 degraded samples and the reference samples were attributed to decomposition over time.
119 We interpreted the differences in litter chemistry between UV treatments as the result of
120 UV photodegradation, which includes both *direct* (abiotic photo-oxidation) and *indirect*
121 (enhancement of microbial decomposition) effects of UV exposure.

122

123 **Materials and methods**

124 Litter samples of *Bromus diandrus* were exposed to two levels of UV radiation at the
125 University of California's Sedgwick Reserve in Santa Ynez, California, USA (43°42'N,
126 120°2'W, approximately 35 km northwest of Santa Barbara, California). The site is
127 dominated by European annual grasses, including *B. diandrus*. The site experiences a
128 Mediterranean climate with alternating hot, dry summers from May to October and cool,
129 rainy winters from November through April. *Bromus* species are commonly found in
130 temperate climates across the world, and many of them are considered to be invasive in
131 North America (D'Antonio and Vitousek 1992). Steel frames with plastic louvers that
132 either pass or block UV radiation (UV-pass or UV-block treatments) were used to
133 manipulate UV radiation received by grass litter. These frames were effective in

134 manipulating UV radiation and allowed penetration of rainfall. There was no difference
135 in air temperature or relative humidity between UV-pass and UV-block treatments. A
136 detailed description of the frames, including dimensions, placement, and optical
137 characteristics, is provided by Lin and King (2014). Litter samples (leaves and stems)
138 were exposed to UV treatments in the field for two durations (2.5 months and one year).
139 For samples with 2.5 months of UV exposure, UV-pass and UV-block screens ($n = 10$)
140 were placed above naturally senesced *B. diandrus* litter from mid August to late October,
141 2011 to capture short-term UV effects during the dry season. Only litter from the very top
142 of the litter layer was collected because this litter was consistently exposed to solar
143 radiation. Approximately 5 g of litter were collected from underneath each screen. For
144 litter with one year of UV exposure, recently senesced litter was collected from the field
145 site in July 2011, placed in aluminum mesh bags, and suspended 5 cm under the UV-pass
146 and UV-block screens (above the litter layer; $n = 10$) from late August 2011 to early
147 September 2012 to capture longer-term UV effects. Mass loss data of this set of litter
148 samples were reported in Lin and King (2014). There were 5 g of litter in each mesh bag
149 before the field exposure, and approximately 4 g remained after one year of field
150 exposure. Although aluminum mesh bags were only used for litter with one year of UV
151 treatment and not for the litter exposed for 2.5 months, one year of UV-pass treatment
152 still resulted in 2.5-fold higher UV exposure than 2.5 months of UV-pass treatment (183
153 MJ/m² vs. 49 MJ/m²). We use these two sets of litter to represent two different dosages of
154 UV radiation. For the reference material (time 0), approximately 5 g of recently senesced
155 litter was collected in July 2011 from each of 10 randomly-selected plots in an open area,

156 adjacent to the UV treatment site. The reference material was stored in the dark under
157 laboratory conditions until further analysis.

158 After UV treatments, litter samples were collected from the field, sorted to remove
159 green plants, arthropods, and visible dust, oven-dried for two days at 55 °C, and ground
160 using a mini Wiley mill with US standard #20 mesh (Thomas Scientific, Swedesboro,
161 New Jersey, USA). To quantify litter fiber fractions, ground subsamples (~0.5 g) were
162 analyzed by a sequential digestion procedure (Van Soest 1963; n = 10; Type 200 Fiber
163 Analyzer, ANKOM Technology, Macedon, New York, USA), hereafter referred to as
164 “fiber analysis.” The fiber fractions include the “cell solubles” (soluble carbohydrates,
165 proteins, and lipids), hemicelluloses, cellulose, and lignin fractions. Because no mass loss
166 data were available for litter with 2.5-months of exposure, we can not report changes in
167 fiber fractions on a mass basis; instead, we report the proportions of fiber fractions in
168 percentages.

169 The 2D ^1H - ^{13}C HSQC NMR spectroscopy was used to characterize the lignin
170 composition and structure of litter cell walls following the protocol described in Kim and
171 Ralph (2010) and Mansfield et al. (2012). In short, for a subset of samples ($n = 3$), 1 g of
172 ground litter tissue was sequentially extracted with water, 80% (vol/vol) ethanol, and
173 acetone. Each solvent extraction was repeated three times for a total of nine extractions.
174 These extractions remove soluble compounds (e.g. starch, protein, and polyphenols) that
175 may distort the examination of cell wall material. During our extraction procedure for the
176 2D NMR analysis, some soluble lignin and hemicellulose-derived compounds were
177 removed, and their responses to time and UV treatments were not examined here. A
178 subsample of the extracted cell wall material (~250 mg) was ground again using a ball

179 mill (Planetary Micro Mill Pulverisette 7 premium line, Fritsch, Idar-Oberstein,
180 Germany) with 20 ml zirconium dioxide (ZrO₂) grinding jars and ten 10-mm ZrO₂ ball
181 bearings in each jar for 45 min (5 min pause with every 5 min grinding; actual grinding
182 time, 25 min). Then, 30 mg of ball-milled isolated cell wall material was transferred to a
183 5-mm NMR tube, followed by 500 µl of pre-mixed 4:1 dimethylsulfoxide (DMSO-
184 *d*₆)/pyridine-*d*₅ (vol/vol). The NMR tubes were sonicated until cell wall material and
185 solvent formed a gel. The 2D ¹H–¹³C HSQC NMR spectra were acquired on a Bruker
186 AVANCE 500 Spectrometer (500 MHz; Rheinstetten, Germany) with a cryogenically-
187 cooled triple-resonance inverse NMR probe. The detailed set-up of NMR experiments
188 can be found in Mansfield et al. (2012). NMR spectral were processed using Bruker’s
189 Topspin 3.1 software.

190 Resonance assignments were confirmed with the “NMR database of lignin and cell
191 wall model compounds” (Ralph et al. 2004) and additional references (Kim and Ralph
192 2010; Talbot et al. 2011; Yelle et al. 2013). Relative abundances of lignin syringyl (S),
193 guaiacyl (G), and *p*-hydroxyphenyl (H) units were determined by integrating S-2/6, G-2,
194 and H-2/6 C–H correlations in the aromatic region of the 2D NMR spectra, respectively
195 (Fig. 1d-f; 7.0/100-8.3/150 ppm). Lignin methoxyl (OMe), the α-position of the lignin β-
196 aryl-ether (L_{Aα}), and acetylated xylan units (2-*O*-Ac-β-D-Xylp and 3-*O*-Ac-β-D-Xylp)
197 were also integrated in the aliphatic region of the 2D NMR spectra (Fig. 1a-c; 2.7/50-
198 6.0/95 ppm). Integration regions for the above features can be found in Supplementary
199 Table 1. Abundances of L_{Aα}, 2-*O*-Ac-β-D-Xylp, and 3-*O*-Ac-β-D-Xylp were evaluated by
200 dividing their integrals by the integral of OMe, as OMe was found to be relatively stable
201 during acid and enzymatic degradation (Lundquist and Lundgren 1972; Yelle et al. 2013).

202 A student's T-test was used to compare effects of UV treatments on fiber fractions and
203 cell wall chemical features at each exposure duration (SPSS 20, IBM Corporation).
204 Before using the T-test, the data were checked for equality of variances using Levene's
205 test. If equal variances could not be assumed, the degrees of freedom of the T-statistic
206 were adjusted using the Welch-Satterthwaite method.

207

208 **Results and Discussion**

209 Litter fiber composition was significantly altered over time (Table 1). The fraction of
210 litter hemicellulose, averaged across the two UV treatments, decreased from 31.6% in the
211 reference material to 28.6% and 24.9% after 2.5 months (T-test, $P < 0.001$, $df = 28$) and
212 one year of decomposition (T-test, $P < 0.001$, $df = 28$), respectively. Across the two UV
213 treatments, the fraction of cell solubles increased from 25.5% in the reference material to
214 28.6% and 33.1% after 2.5 months (T-test, $P < 0.001$, $df = 28$) and one year of
215 decomposition (T-test, $P < 0.001$, $df = 28$), respectively. These changes over time were
216 larger in magnitude than changes induced by UV exposure. For litter exposed for 2.5
217 months, there were no significant effects of UV treatment except for a marginally
218 significant effect of UV exposure on the cellulose fraction (T-test, $P = 0.086$, $df = 18$).
219 For litter exposed for one year, all four fiber fractions were affected by UV treatments,
220 but the change in hemicellulose fraction was the greatest in magnitude. The hemicellulose
221 fraction was smaller in the UV pass compared to the UV block treatment (23.8% vs.
222 25.9%; T-test, $P < 0.001$, $df = 18$); cell solubles, cellulose, and lignin fractions were all
223 higher in the UV pass treatment.

224 Compared to the reference sample, degraded samples had broadened contours along
225 the proton dimension of the 2D NMR spectra (Figure 1). This phenomenon could be
226 induced by inclusion of dust and soil particles or association with metals; however, it is
227 commonly indicative of degradation of plant samples caused by enzymes, hydrothermal
228 treatments, and acids (Samuel et al. 2011; Yelle et al. 2013). Therefore, it is likely that
229 the chemical complexity of litter cell wall material increased after field decomposition
230 relative to the already complex but nevertheless well-defined and limited structural types
231 in the native cell wall. Further studies are needed to verify these hypotheses.

232 Aromatic regions of the NMR spectra showed that lignin syringyl (S) and guaiacyl
233 (G) units were much more abundant than *p*-hydroxyphenyl (H) units in this grass material
234 (Fig. 1d). Integration of lignin units showed that the abundance of G units decreased from
235 60% in the reference material to 52% across the two UV treatments after one year (Table
236 1, Fig. 1e and f; T-test, $P = 0.005$, $df = 7$), which corresponded to increases in S units (T-
237 test, $P = 0.005$, $df = 7$) and to marginal increases in H units (T-test, $P = 0.075$, $df = 7$).
238 The UV treatments did not affect levels of S and G units; however, it marginally
239 decreased abundance of H units after 2.5 months (T-test, $P = 0.058$, $df = 4$) and one year
240 (T-test, $P = 0.066$, $df = 4$). These results suggest that lignin structure underwent
241 significant changes during one year of decomposition, and effects of UV
242 photodegradation were small relative to those that occurred over time.

243 Aliphatic regions of the NMR spectra showed that β -aryl ethers ($L_{A\alpha}$) were the
244 dominant linkage among lignin units (Fig. 1a-c). A small phenylcoumaran (L_B) signal
245 was present in the reference sample, but not in degraded samples, suggesting that L_B
246 linkages were vulnerable to decomposition. Integration results showed that levels of $L_{A\alpha}$

247 did not change over time, but one year of UV-pass treatment had 9% lower $L_{A\alpha}$ linkages
248 than the UV-block treatment (Fig. 2a: T-test, $P = 0.047$, $df = 4$). This result suggests that
249 the β -aryl ether linkages are degraded upon exposure to UV radiation, which is consistent
250 with previous studies on photodegradation of wood lignin (Argyropoulos and Sun 1996;
251 Lanzalunga and Bietti 2000). It is unclear why the levels of 3-*O*-Ac- β -D-Xylp were
252 higher in degraded samples than in the reference material, but one year of the UV-pass
253 treatment had less 2-*O*-Ac- β -D-Xylp (Fig. 2b: T-test, $P = 0.014$, $df = 4$) and marginally
254 fewer 3-*O*-Ac- β -D-Xylp units (Fig. 2c: T-test, $P = 0.083$, $df = 4$) than the UV-block
255 treatment. These reductions in xylan features were consistent with the fiber analysis result
256 showing that UV exposure reduced the hemicellulose fraction (Table 1). These results
257 indicate that exposure to UV radiation induced degradation of lignin and hemicelluloses.

258 Both fiber analysis and 2D NMR spectroscopy showed that changes in litter
259 chemistry over time were more prominent than those induced by UV treatments (Table
260 1). This result is not surprising given that many previous field experiments have shown a
261 significant but small contribution of photodegradation to overall litter mass loss
262 (reviewed by King et al. 2012). In our study, microbial decomposition was likely
263 responsible for the majority of changes in litter chemistry over time, despite the fact that
264 litter samples were not in direct contact with soil. For example, microorganisms may
265 have come in contact with the litter through aeolian transport, and endophytes that live
266 within the litter could also have contributed to decomposition. Microbial decomposition
267 of litter could have been sustained by atmospheric water vapor in our Mediterranean
268 climate, without water input from soil (Dirks et al. 2010). Therefore, our results indicate

269 that UV photodegradation has a small effect on litter chemistry compared to microbial
270 decomposition.

271 The 2D NMR spectroscopy data demonstrate that UV exposure degraded the
272 dominant inter-unit linkages in β -aryl ethers and lignin H units (Table 1 and Fig. 2a).
273 Although the fiber analysis suggests that the lignin fraction was higher with UV pass
274 compared to UV block after one year (Table 1), this increase in lignin fraction could
275 simply be a reflection of the loss of hemicellulose or accumulation of microbial by-
276 products (Cou[^]teaux et al. 1995). Together, these data suggest that photodegradation
277 weakens the lignin structure but may not completely break down lignin molecules. This
278 pattern of partial degradation of lignin structure might explain results in previous studies
279 that reported no responses of lignin content to UV treatments (Baker and Allison 2015;
280 Brandt et al. 2010; Kirschbaum et al. 2011). More importantly, this pattern represents an
281 important mechanism through which solar radiation may increase exposure of cell wall
282 compounds to extracellular enzymes and consequently increase litter biodegradability
283 (i.e. photo-priming, Bornman et al. 2015; Foereid et al. 2010; Wang et al. 2015). Photo-
284 priming may occur during radiation exposure (e.g. this study; Baker and Allison 2015) or
285 after the incorporation of litter into the soil (Foereid et al. 2010). Overall, our 2D NMR
286 spectroscopy data offer novel empirical evidence to support the photo-priming hypothesis
287 (Bornman et al. 2015).

288 In addition to effects on lignin structure, both fiber analysis and 2D NMR
289 spectroscopy results support the idea that UV exposure degraded hemicellulose structure
290 (Table 1 and Fig. 2). This result falls in line with findings from several field experiments
291 (Baker and Allison 2015; Brandt et al. 2010; Brandt et al. 2007). However, mechanisms

292 behind abiotic photo-oxidation of hemicellulose, such as acetylated xylan, are less studied
293 (except Yamagishi et al. 1970). Previous studies of cellulose acetate offer key insights
294 into the photodegradation processes of acetylated xylan, because these two compounds
295 are structurally analogous. Both compounds can be degraded by microbial carbohydrate
296 esterases (Biely 2012; Puls et al. 2011), and UV exposure has been found to increase
297 enzymatic degradation of cellulose acetate (Ishigaki et al. 2002; Jang et al. 2007).
298 Therefore, it is likely that UV radiation facilitated microbial degradation of acetylated
299 xylan (Fig. 2). Thus, photo-oxidation of acetylated xylan would be a second mechanism
300 through which UV radiation may increase litter biodegradability.

301 Results from 2D NMR spectroscopy demonstrate that the relative abundance of lignin
302 G units decreased significantly after one year of field decomposition, which is consistent
303 with several studies that reported preferential loss of G units during early stages of litter
304 decomposition (Christmas and Oglesby 1971; Kögel 1986; Quideau et al. 2005).
305 However, other studies have found slower loss of G units relative to other lignin units,
306 especially during later stages in litter decomposition (Bahri et al. 2006; Bertrand et al.
307 2006; Talbot et al. 2011), suggesting that changes in lignin G units during decomposition
308 likely depend on the stage of decomposition and also on the species of litter material.

309 In conclusion, we found significant loss of hemicelluloses and lignin G units of *B.*
310 *diandrus* litter over one year of field decomposition, driven primarily by microbial
311 decomposition. Exposure to UV radiation induced partial lignin degradation that was
312 evidenced by loss of β -aryl ethers and lignin H units, but was not apparent as a change in
313 lignin fraction. Our results indicate that UV photodegradation has a small but significant
314 effect on litter chemistry compared to microbial decomposition. These data suggest that

315 degradation of lignin and hemicelluloses are important pathways through which UV
316 radiation increases litter degradability. Our study also demonstrates the effectiveness of
317 2D NMR spectroscopy in obtaining detailed comparative information about litter
318 chemical composition that can lead to a better understanding of decomposition processes
319 and C cycling in general.

320

321 **Acknowledgements**

322 We thank Dad Roux-Michollet, Keri Opalk, Sarah Liu, and Jerry Hu for their assistance
323 in the field and laboratory. We thank Oliver Chadwick and Carla D'Antonio for their
324 valuable comments on the experimental design and on this manuscript. We thank Kate
325 McCurdy, Eric Massey, and the University of California's Sedgwick Reserve for
326 providing the study site. Comments from Associate Editor Marc Kramer and four
327 anonymous reviewers greatly improved this manuscript. YL and JK were supported by
328 the National Science Foundation under DEB-0935984 and DEB-1406501. JR and SK
329 were supported by the DOE Great Lakes Bioenergy Research Center (DOE Office of
330 Science BER DE-FC02-07ER64494).

331

332 **References**

333 Adair EC, Parton WJ, Del Grosso SJ, Silver WL, Harmon ME, Hall SA, Burke IC, Hart
334 SC (2008) Simple three - pool model accurately describes patterns of long - term
335 litter decomposition in diverse climates. *Global Change Biol* 14: 2636-2660
336 Aerts R (1997) Climate, leaf litter chemistry and leaf litter decomposition in terrestrial
337 ecosystems: a triangular relationship. *Oikos*: 439-449
338 Amin BAZ, Chabbert B, Moorhead D, Bertrand I (2014) Impact of fine litter chemistry
339 on lignocellulolytic enzyme efficiency during decomposition of maize leaf and
340 root in soil. *Biogeochemistry* 117: 169-183
341 Argyropoulos DS, Sun Y (1996) Photochemically induced solid-state degradation,
342 condensation, and rearrangement reactions in lignin model compounds and milled
343 wood lignin. *Photochem Photobiol* 64: 510-517

344 Austin AT, Ballaré CL (2010) Dual role of lignin in plant litter decomposition in
345 terrestrial ecosystems. *Proc Natl Acad Sci USA* 107: 2-6

346 Bahri H, Dignac M-F, Rumpel C, Rasse DP, Chenu C, Mariotti A (2006) Lignin turnover
347 kinetics in an agricultural soil is monomer specific. *Soil Biol Biochem* 38: 1977-
348 1988

349 Baker NR, Allison SD (2015) Ultraviolet photodegradation facilitates microbial litter
350 decomposition in a Mediterranean climate. *Ecology* 96: 1994-2003

351 Bertrand I, Chabbert B, Kurek B, Recous S (2006) Can the biochemical features and
352 histology of wheat residues explain their decomposition in soil? *Plant Soil* 281:
353 291-307

354 Biely P (2012) Microbial carbohydrate esterases deacetylating plant polysaccharides.
355 *Biotechnol Adv* 30: 1575-1588

356 Bornman JF, Barnes PW, Robinson SA, Ballare CL, Flint SD, Caldwell MM (2015)
357 Solar ultraviolet radiation and ozone depletion-driven climate change: effects on
358 terrestrial ecosystems. *Photochemical & Photobiological Sciences* 14: 88-107

359 Brandt LA, Bohnet C, King JY (2009) Photochemically induced carbon dioxide
360 production as a mechanism for carbon loss from plant litter in arid ecosystems. *J*
361 *Geophys Res-Bioge* 114: G02004

362 Brandt LA, King JY, Hobbie SE, Milchunas DG, Sinsabaugh RL (2010) The role of
363 photodegradation in surface litter decomposition across a grassland ecosystem
364 precipitation gradient. *Ecosystems* 13: 765-781

365 Brandt LA, King JY, Milchunas DG (2007) Effects of ultraviolet radiation on litter
366 decomposition depend on precipitation and litter chemistry in a shortgrass steppe
367 ecosystem. *Global Change Biol* 13: 2193-2205

368 Christmas RF, Oglesby RT (1971) Microbiological degradation and the formation of
369 humus.

370 Couˆteaux M-M, Bottner P, Berg B (1995) Litter decomposition, climate and litter quality.
371 *Trends Ecol Evol* 10: 63-66

372 D'Antonio CM, Vitousek PM (1992) Biological invasions by exotic grasses, the grass/fire
373 cycle, and global change. *Annu Rev Ecol Syst*: 63-87

374 Dirks I, Navon Y, Kanas D, Dumbur R, Grünzweig J (2010) Atmospheric water vapor as
375 driver of litter decomposition in Mediterranean shrubland and grassland during
376 rainless seasons. *Global Change Biol* 16: 2799-2812

377 Feng X, Hills KM, Simpson AJ, Whalen JK, Simpson MJ (2011) The role of
378 biodegradation and photo-oxidation in the transformation of terrigenous organic
379 matter. *Org Geochem* 42: 262-274

380 Foereid B, Bellarby J, Meier-Augenstein W, Kemp H (2010) Does light exposure make
381 plant litter more degradable? *Plant Soil* 333: 275-285

382 Frouz J, Cajthaml T, Mudrak O (2011) The effect of lignin photodegradation on
383 decomposability of *Calamagrostis epigeios* grass litter. *Biodegradation* 22: 1247-
384 1254

385 George B, Suttie E, Merlin A, Deglise X (2005) Photodegradation and photostabilisation
386 of wood - the state of the art. *Polym Degradation Stab* 88: 268-274

387 Ishigaki T, Sugano W, Ike M, Taniguchi H, Goto T, Fujita M (2002) Effect of UV
388 irradiation on enzymatic degradation of cellulose acetate. *Polym Degradation Stab*
389 78: 505-510

390 Jang J, Lee H, Lyoo W (2007) Effect of UV irradiation on cellulase degradation of
391 cellulose acetate containing TiO₂. *Fiber Polym* 8: 19-24
392 Kim H, Ralph J (2010) Solution-state 2D NMR of ball-milled plant cell wall gels in
393 DMSO-d₆/pyridine-d₅. *Org Biomol Chem* 8: 576-591
394 Kim H, Ralph J, Akiyama T (2008) Solution-state 2D NMR of ball-milled plant cell wall
395 gels in DMSO-d₆. *Bioenerg Res* 1: 56-66
396 King JY, Brandt LA, Adair EC (2012) Shedding light on plant litter decomposition:
397 advances, implications and new directions in understanding the role of
398 photodegradation. *Biogeochemistry* 111: 57-81
399 Kirschbaum MUF, Lambie SM, Zhou H (2011) No UV enhancement of litter
400 decomposition observed on dry samples under controlled laboratory conditions.
401 *Soil Biol Biochem* 43: 1300-1307
402 Kögel I (1986) Estimation and decomposition pattern of the lignin component in forest
403 humus layers. *Soil Biol Biochem* 18: 589-594
404 Lanzalunga O, Bietti M (2000) Photo- and radiation chemical induced degradation of
405 lignin model compounds. *Photochem Photobiol* 56: 85-108
406 Lee H, Rahn T, Throop H (2012) An accounting of C-based trace gas release during
407 abiotic plant litter degradation. *Global Change Biol* 18: 1185-1195
408 Lundquist K, Lundgren R (1972) Acid degradation of lignin. *Acta Chem Scand* 26: 2005-
409 2023
410 Mansfield SD, Kim H, Lu F, Ralph J (2012) Whole plant cell wall characterization using
411 solution-state 2D NMR. *Nat Protoc* 7: 1579-1589
412 Mayer LM, Thornton KR, Schick LL, Jastrow JD, Harden JW (2012) Photodissolution of
413 soil organic matter. *Geoderma* 170: 314-321
414 Melillo JM, Aber JD, Muratore JF (1982) Nitrogen and lignin control of hardwood leaf
415 litter decomposition dynamics. *Ecology* 63: 621-626
416 Moore TR, Trofymow JA, Taylor B, Prescott C, Camire C, Duschene L, Fyles J, Kozak
417 L, Kranabetter M, Morrison I (1999) Litter decomposition rates in Canadian
418 forests. *Global Change Biol* 5: 75-82
419 Parton W, Silver WL, Burke IC, Grassens L, Harmon ME, Currie WS, King JY, Adair
420 EC, Brandt LA, Hart SC (2007) Global-scale similarities in nitrogen release
421 patterns during long-term decomposition. *Science* 315: 361-364
422 Petrik DL, Karlen SD, Cass CL, Padmakshan D, Lu F, Liu S, Le Bris P, Antelme S,
423 Santoro N, Wilkerson CG, Sibout R, Lapierre C, Ralph J, Sedbrook JC (2014) p-
424 Coumaroyl-CoA:monolignol transferase (PMT) acts specifically in the lignin
425 biosynthetic pathway in *Brachypodium distachyon*. *Plant J* 77: 713-726
426 Puls J, Wilson SA, Hölter D (2011) Degradation of cellulose acetate-based materials: a
427 review. *J Polym Environ* 19: 152-165
428 Quideau SA, Graham RC, Oh SW, Hendrix PF, Wasylishen RE (2005) Leaf litter
429 decomposition in a chaparral ecosystem, Southern California. *Soil Biol Biochem*
430 37: 1988-1998
431 Ralph SA, Ralph J, Landucci LL (2004) NMR database of lignin and cell wall model
432 compounds. November 2004. Available at URL
433 <http://ars.usda.gov/Services/docs.htm?docid=10491>

434 Samuel R, Foston M, Jiang N, Allison L, Ragauskas AJ (2011) Structural changes in
435 switchgrass lignin and hemicelluloses during pretreatments by NMR analysis.
436 *Polym Degradation Stab* 96: 2002-2009

437 Schade GW, Hofmann R-M, Crutzen PJ (1999) CO emissions from degrading plant
438 matter: (I). Measurements. *Tellus (B Chem Phys Meteorol)* 51: 889-908

439 Schaefer D, Steinberger Y, Whitford WG (1985) The failure of nitrogen and lignin
440 control of decomposition in a North American desert. *Oecologia* 65: 382-386

441 Song X, Peng C, Jiang H, Zhu Q, Wang W (2013) Direct and indirect effects of UV-B
442 exposure on litter decomposition: a meta-analysis. *PloS One* 8: e68858

443 Talbot JM, Yelle DJ, Nowick J, Treseder KK (2011) Litter decay rates are determined by
444 lignin chemistry. *Biogeochemistry* 108: 279-295

445 Van Soest PJ (1963) Use of detergents in analysis of fibrous feeds: a rapid method for the
446 determination of fiber and lignin. *J Ass Offic Agr Chem* 46: 829-835

447 Wang J, Liu L, Wang X, Chen Y (2015) The interaction between abiotic
448 photodegradation and microbial decomposition under ultraviolet radiation. *Global*
449 *Change Biol* 21: 2095-2104

450 Wilkerson CG, Mansfield SD, Lu F, Withers S, Park JY, Karlen SD, Gonzales-Vigil E,
451 Padmakshan D, Unda F, Rencoret J, Ralph J (2014) Monolignol ferulate
452 transferase introduces chemically labile linkages into the lignin backbone. *Science*
453 344: 90-93

454 Yamagishi T, Yoshimoto T, Minami K (1970) Photodegradation of wood. VII. Isolation
455 and photodegradation of O-acetylated xylan (hemicellulose) from Linden wood. *J*
456 *Jpn Wood Res Soc* 16: 87-91

457 Yelle DJ, Kaparaju P, Hunt CG, Hirth K, Kim H, Ralph J, Felby C (2013) Two-
458 Dimensional NMR evidence for cleavage of lignin and xylan substituents in
459 wheat straw through hydrothermal pretreatment and enzymatic hydrolysis.
460 *Bioenerg Res* 6: 211-221

461

462 Table 1. Effects of UV radiation exposure and time of exposure on litter fiber fractions ($n = 10$, percentages by mass, fiber analysis)
 463 and lignin units ($n = 3$, percentages by mass, 2D NMR spectroscopy).

	Reference litter*	Exposure time					
		2.5 months			1 year		
		UV-pass	UV-block	P^\dagger	UV-pass	UV-block	P
Fiber fractions							
% Cell solubles	25.5 (0.6)	28.5 (0.7)	28.7 (0.7)	n.s.	33.4 (0.3)	32.7 (0.3)	0.099
% Hemicelluloses	31.6 (0.3)	28.5 (0.5)	28.7 (0.5)	n.s.	23.8 (0.3)	25.9 (0.3)	< 0.001
% Cellulose	39.7 (0.5)	39.8 (0.3)	39.0 (0.3)	0.086	38.8 (0.2)	37.9 (0.3)	0.018
% Lignin	3.2 (0.2)	3.3 (0.2)	3.6 (0.2)	n.s.	4.0 (0.2)	3.5 (0.2)	0.068
Lignin units‡							
% Syringyl (S)	34.5 (1.2)	33.2 (2.0)	33.4 (1.6)	n.s.	39.9 (1.6)	41.4 (0.6)	n.s.
% Guaiacyl (G)	60.0 (0.8)	60.8 (2.4)	59.4 (1.7)	n.s.	53.8 (2.0)	50.7 (1.0)	n.s.
% <i>p</i> -Hydroxyphenyl (H)	5.5 (0.6)	6.0 (0.4)	7.2 (0.1)	0.058	6.3 (0.4)	7.9 (0.5)	0.066

464

Notes: Values are means with S.E. in parentheses. Bold results indicate significant differences at $\alpha = 0.05$ level.

* See Methods for the definitions of reference litter.

† P values of T-tests between UV treatments in a given exposure time.

‡ Refer to Supplementary Table 1 for the integration areas of the lignin units.

465

466 Figure Captions:

467

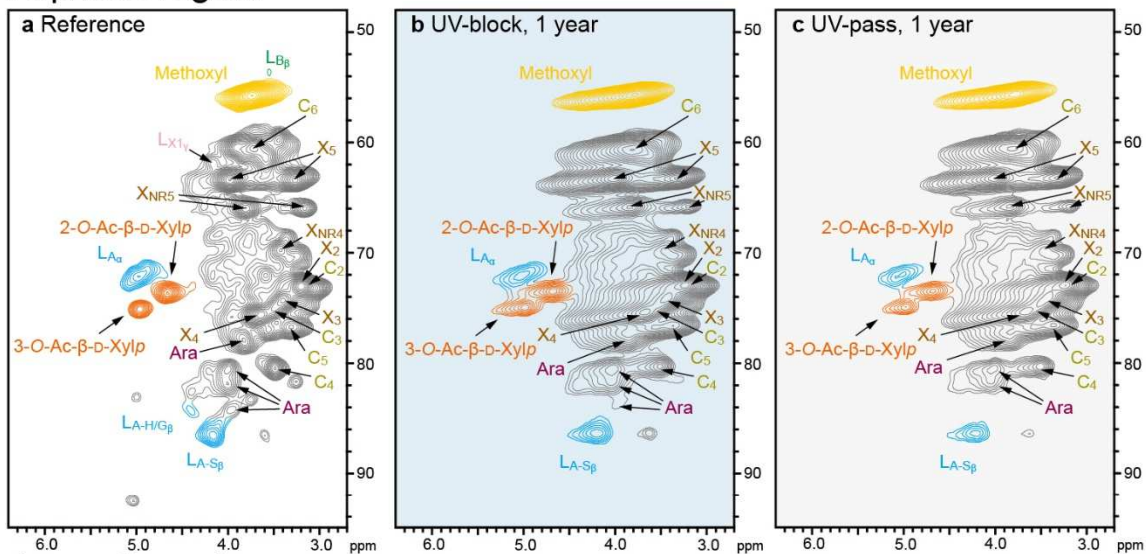
468 Figure 1. 2D ^1H - ^{13}C HSQC NMR spectra of cell wall gel of *Bromus diandrus* litter in 4:1
469 DMSO- d_6 /pyridine- d_5 (vol:vol) in the aliphatic region (**a-c**) and the aromatic region (**d-f**).
470 Spectra are aligned vertically to represent samples from the following treatments:
471 reference, one year of UV-block, and one year of UV-pass. Contours in the aromatic
472 region are integrated to estimate S/G/H ratios. Contours in the aliphatic region are
473 integrated to estimate lignin methoxyl, lignin inter-unit linkage types, and acetylated
474 xylan.

475

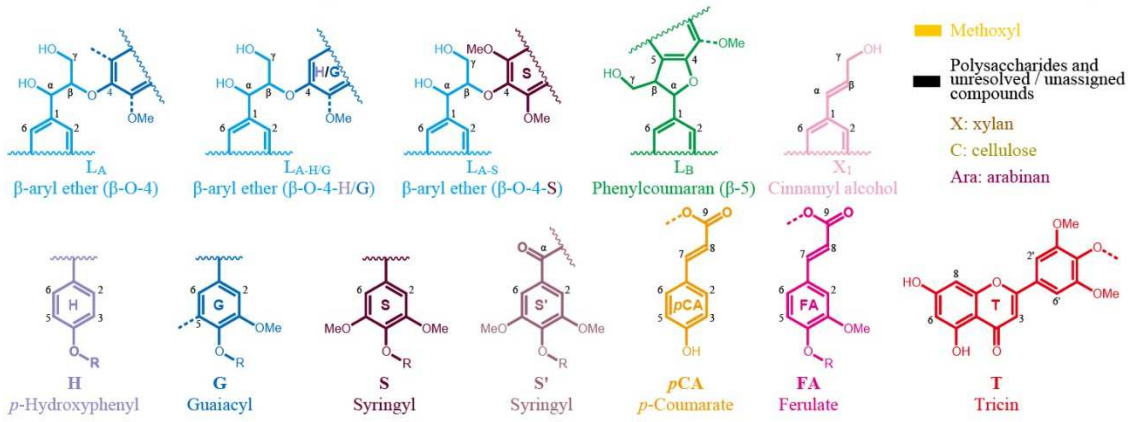
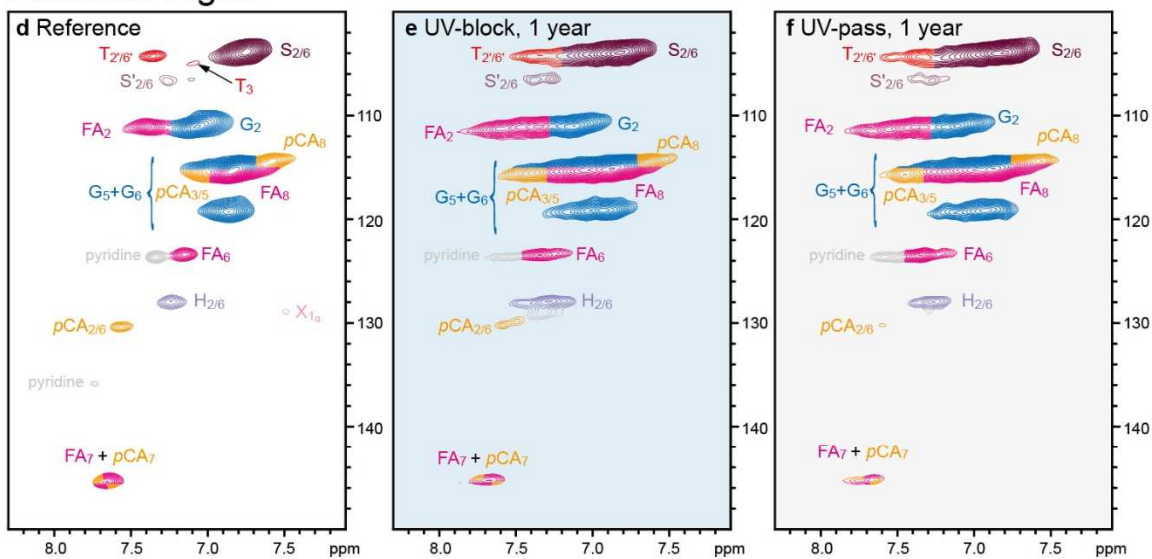
476 Figure 2. Effects of UV treatments (UV-pass, UV-block) and exposure duration on the
477 ratios to lignin methoxyl (OMe) of (**a**) lignin β -aryl ether ($L_{A\alpha}$), (**b**) acetylated xylan (2-
478 *O*-Ac- β -D-Xylp), and (**c**) acetylated xylan (3-*O*-Ac- β -D-Xylp) in *Bromus diandrus* litter.
479 Error bars indicate standard errors ($n = 3$). ** and * indicate statistical differences
480 between UV-pass and UV-block in a given exposure time at $\alpha = 0.05$ and 0.10,
481 respectively. Dotted line indicates the value of measured variable in reference samples
482 that were not exposed to UV treatments ($n = 3$).

483

Aliphatic region

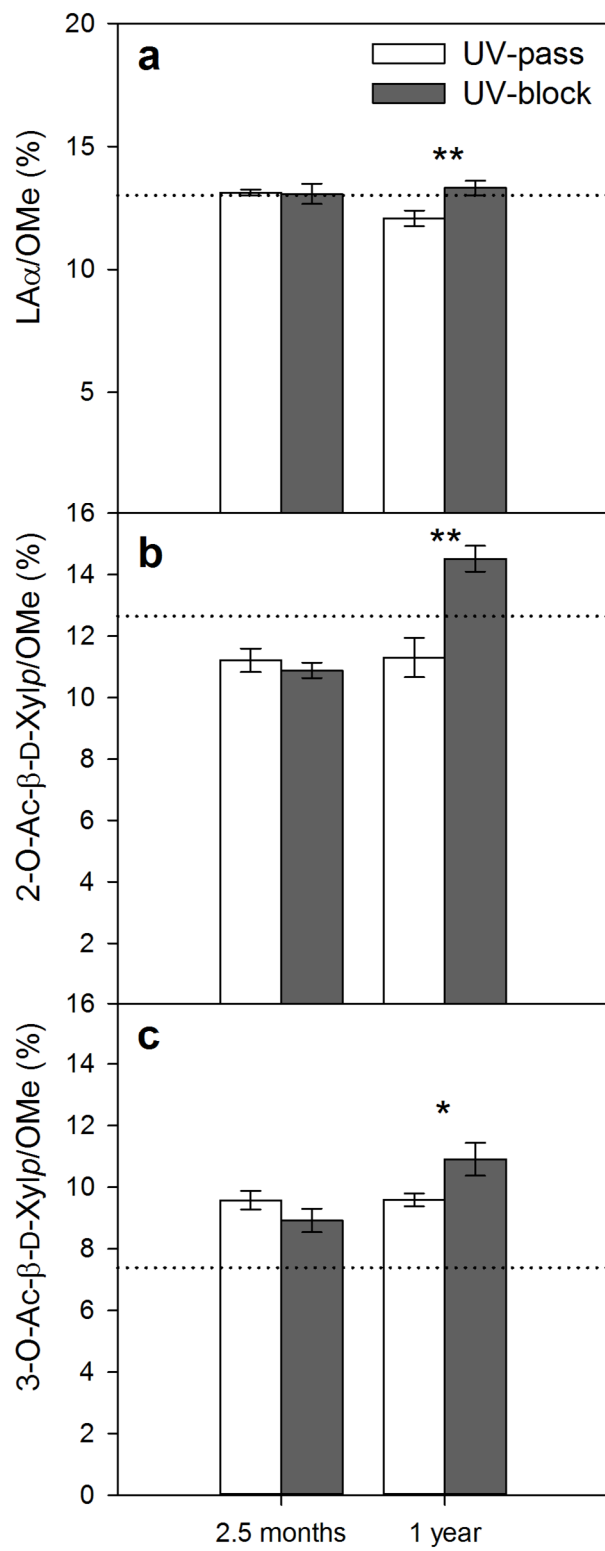


Aromatic region



484

485 Figure 1



486

487 Figure 2

488

489 Supplementary Table 1. 2D NMR contour integration regions for lignin methoxyl (OMe),
490 β -aryl-ether ($L_{A\alpha}$), acetylated xylan units (2-*O*-Ac- β -D-Xylp and 3-*O*-Ac- β -D-Xylp), and
491 syringyl ($S_{2/6}$ and $S'_{2/6}$), guaiacyl (G_2), and *p*-hydroxyphenyl ($H_{2/6}$) lignin units.

Structure	^{13}C ppm	^1H ppm
OMe	57.2-54.3	4.02-3.36
$L_{A\alpha}$	73.4-70.4	5.15-4.79
2- <i>O</i> -Ac- β -D-Xylp	74.8-72.4	4.78-4.50
3- <i>O</i> -Ac- β -D-Xylp	76.1-74.0	5.08-4.84
$S_{2/6}$	105.6-102.0	7.03-6.56
$S'_{2/6}$	107.6-105.7	7.41-7.04
G_2	112.6-108.8	7.25-6.80
$H_{2/6}$	129.1-126.9	7.35-7.10

492

493

494